

Green Synthesis of Doped and Undoped Zinc Oxide Nanoparticles using Aloe vera Extract and Nanocomposites with Reduced Graphene Oxide for Facile Photo Catalytic Degradation of Ponceau 4R Dye : Kinetic Study with Dopants Effect.

¹R.Vijayalakshmi, ²L.Ramapriya and ³J.Santhanalakshmi

¹,Department of Chemistry, Quaid E Millath Government College for Women, Annasalai, Chennai 600 002, TamilNadu, India

²Department of Chemistry, Dr.M.G.R Educational and Research Institute, Chennai 600 095, TamilNadu, India

³Department of Physical Chemistry, University of Madras, Maraimalai Campus, Chennai – 600 025 (Retd.)

DOI: 10.29322/IJSRP.13.12.2023.p14412

<https://dx.doi.org/10.29322/IJSRP.13.12.2023.p14412>

Paper Received Date: 12th October 2023

Paper Acceptance Date: 26th November 2023

Paper Publication Date: 6th December 2023

Abstract- Metal/metal oxide- reduced graphene oxide nanocomposites are widely and partially used as reaction catalysts, photo catalyst, electrode coats, sensors, adsorbents etc. It is possible to synthesize such nanocomposites adopting eco-friendlier green pathways. In the present work, Zinc Oxide nanoparticles are prepared using Aloe Vera plant extract as the stabilizing agent in mild hydrothermal conditions. Adopting similar conditions, 5 mol% dopant metal ion such as Mg(II), Cu(II), Mn(II), Ni(II) and Sb(II) are included and doped ZnO nps are prepared. powder XRD and HR-TEM measurements are carried out for size determinations. Using modified Hummers method and ultrasonication, graphite powder and doped and undoped ZnO nps are used in the nanocomposite preparations. In this process eco friendlier solvents and mild hydrothermal conditions have been adopted, HR TEM photos of the nanocomposites with undoped and doped ZnO nps are measured. The band gap energy (eV) values of the ZnO nps in the as-synthesized forms are known from the Tauc plots. To understand the photo catalytic behavior photo oxidative degradation studies on Ponceau 4R dye which is widely used in food and beverage industry was undertaken. During the progress of the dye degradation under UV irradiation, absorbance variation with time data are collected from the visible spectra of the dye solution scanned at intervals of time. The photo catalysis of the dye solution was performed in the presence of undoped and doped ZnO nps-rGO nanocomposites as catalysts separately adopting similar conditions. From the kinetic plots, the overall pseudo first order rate coefficient values of the dye degradations for each of photo catalysts are found out. Based on the experimental data, the correlations with the effects of band gap variations, nanosizes, and photo catalytic behavior of the ZnO nps – rGO nanocomposites are evaluated. Ni(II) doped ZnO nps nanocomposites produced more rapid dye degradation under UV irradiation than the other doped and undoped ZnO nps nanocomposites.

Index Terms- Ponceau 4R dye degradation photo catalysis, doped ZnOnps with dopantions Mg(II), Cu(II), Mn(II), Ni(II) and Sb(II), ZnO nps- rGO nanocomposites as photo catalysts.

I. INTRODUCTION

Inflow of dye pollutants into environmental water sources has been always on the increase, due to efficient discharges from industries involving textile dyeing, food colorants, paints, printings, cosmetics, beverages, leather products etc which are certainly everlasting[1-6].Hence, currently many advanced oxidation processes (AOPs) are involved in the treatment of industrial dye waste waters. One of the widely used AOPs is the photo degradation process involving photocatalytic nanomaterials [7-10]. At present, Zinc Oxide nanoparticles (ZnO nps) [11-20], stand next inline to TiO₂ nanoparticles in the photocatalytic processes because ZnO nps exhibit eco benign properties, cost effectiveness, abundancy, non- toxicity and band gap E_g (3.36eV) being similar to anatase TiO₂ E_g (3.2eV) [21-23]. In this work, ZnO nps are synthesized adopting green chemistry method, by using Aloe vera plant extract as the stabilizing agent instead of synthetic and polymeric agents and mild aqueous hydrothermal conditions [24,25].

The as – synthesized ZnO nps are size characterized form powder XRD, HR – TEM and E_g measurements. ZnO nps synthesized by green chemistry pathway in this work, show a band gap, E_g equals to 3.367eV. This indicate that ZnO nps in as-synthesised condition is suitable for photocatalyst activity. However it has been reported that, in UV light, recombination of photo generated electron (e⁻) and hole (h⁺) occurs rapidly causing retardation in photoactivity. Among the nano materials, reduced graphene oxide (rGO) possesses E_g as 4.42eV which favors nanocompositisation with ZnO nps. ZnO nps-rGO nanocomposites expose improved photo e⁻ transfer to graphene

sheets, thereby minimizing the e^- / h^+ recombination losses. In the present work, ZnO nps synthesized are impregnated onto rGO sheets adopting simple hydrothermal and ultrasonication methods. Also, using graphite powders, and eco- friendlier reagents and mild solution conditions, exfoliated rGO sheets are prepared.

Dopants, consisting of metal (II) ions into ZnO nps play a prominent role in further enhancing the photoactivity by altering the band gap, size quantizations and slender lattice distortions in ZnO nps [26-31]. Also, dopants that bring in enhanced photoactivity in ZnO nps, retard to certain extent the photo recombination steps. Adopting co-precipitation method and in presence of plant Aloe vera extract, doped ZnO nps are prepared with 5 mol% metal(II) ions such as Mg(II),Cu(II),Mn(II), Ni(II) and Sb(II) respectively. The band gap and the nano size of doped ZnO nps are determined using Tauc plots and powder XRD data. All the doped ZnO nps are impregnated into rGO 2D nanosheets adopting similar procedure of ZnO nps-rGO nano composites preparations. In order to confirm the photo catalytic activities of the synthesized undoped and doped ZnO nps-rGO nanocomposites, the photo oxidative degradation of Ponceau 4R dye under UV irradiation has been studied. P 4R is a water soluble synthetic azo dye, its molecular structure shown in **Figure 1** which is used profusely as colouring agent in desserts ,beverages, soft drinks and other foods because of the low price,excellent stability and effectiveness [32,33]. However, its consumption causes migranes, skin allergies, diarrhea, and even carcinogenicity [34-36]. Therefore studies in the treatment of P 4R polluted water will bear societal scientific importance.The kinetics of the photo degradations of the dye are followed from the spectra scan at various time intervals of progress of the reaction. The catalytic activities of the undoped and doped ZnO nps-rGO nanocomposites are compared from the overall pseudo first order rate coefficient values. A suitable mechanism of photo oxidation of the dye Ponceau 4R has been proposed.

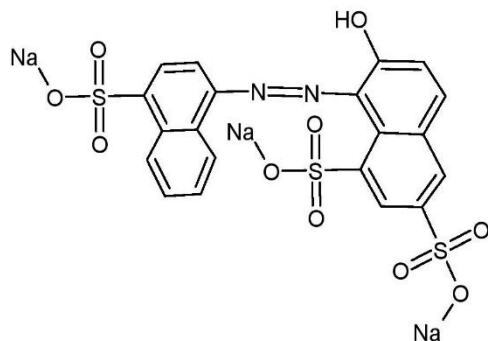


Fig. 1. Molecular structure of Ponceau 4R dye

II. EXPERIMENTAL

2.1 Chemicals

Zinc acetate, Nitrates of Mg(II),Cu(II),Mn(II), Ni(II) and Sb(II) are procured from Merck, India. Graphite powder was purchased from Alfa Aesar. Ethylene glycol, NaOH pellets, $KMnO_4$, Phosphoric acid and Sulfuric acid from SRL, India, Analar grade are used. Fresh triple distilled water was used in all solution preparations.

2.2 Synthesis of ZnO Nanoparticles

Nanocrystalline Zinc Oxide samples are prepared from Zinc acetate aqueous solution. To 50 ml of 1 mM zinc precursor solution and 10 ml of 5 M NaOH and 20 ml of ethylene glycol was added drop wise under vigorous constant stirring for 1 hour, maintaining the solution temperature at 60° C until milky white slurry occurred. The reaction mixture was cooled and ultra centrifuged. The residue was repeatedly washed, centrifuged and vacuum dried. The fresh dry powder was annealed at 600° C for 3 hrs. Regarding, doped ZnO nps, 5 ml of the dopant metal nitrate precursor in 0.5 mM solution, was added initially to the Zinc acetate solution and repeated the procedure as above. For all dopants, 5 mol % addition was maintained. The annealed powder are subjected to characterisations.

2.3 Preparation of rGO nanocomposites

Using graphite powder, graphene oxide (GO) was prepared adopting modified Hummer's method [37-40]. Graphite powder and 2.5 $NaNO_3$ are added to 120 ml concentrated H_2SO_4 and the mixture was cooled to 10°C and further 15 g of $KMnO_4$ was slowly added with slow stirring. Mixture was added 250 ml of triple distilled water with stirring. The solution contents are heated to 70°C for 2hr. At room temperature, 20 ml of 30% w/v H_2O_2 was added with stirring and washed with water and excess acetone. The residue was vacuum dried and heated to 60°C for 2 hrs and stored. Reduced graphene oxide (rGO) was prepared from the GO powder by taking 100mg GO in 50ml triple distilled water 10ml of hydrazine monohydrate was added and stirred at 80°C for 12 hr. The resulting suspension was filtered and the residue was vacuum dried at 80°C for 6hrs.

For the preparation of ZnO nps – rGO nanocomposites, typically 0.5 $mg mL^{-1}$ rGO was dispersed in 100ml of triple distilled water, stirred vigorously and ultrasonicated for exfoliation of rGO sheets. To this suspension, 10 mg of ZnO nps are dispersed and NaOH solution was added till the pH was attained at 10.0. Ultrasonication and maintaining the reaction mixture temperature at 60°C for 3 hrs until the blackish grey slurry was formed.

After ultra centrifugation, the residue was repeatedly washed and vacuum dried at 60°C. This procedure was identically followed for metal (II) ions doped ZnO nps composite impregnation on to rGO, separately for each type of dopants chosen. All the undoped and doped ZnO nps – rGO nanocomposites are stored in argon atmosphere for further use.

2.4 Size Characterisations

The undoped and doped nanocomposite samples are subjected to Powder XRD using Bruker diffractometer D8 Advance with $Cu K\alpha$ radiation. HR-TEM measurements were carried out using TEM Hitachi Technai G20 and for FE-SEM, Hitachi FESEM S4800 microscopes and all visible spectra were recorded on Shimadzu (UV-1650PC) spectrometer fitted with thermostat for temperature control. The band gap values of undoped and doped ZnO nps are found out from UV – Visible diffuse spectra data. Diffuse reflectance UV-VS spectra of pressed powder samples diluted with spectra grade KBr, recorded using Shimadzu UV-3600 spectrometer

2.5 Photo catalytic studies

1 pot batch reactor type fitted with temperature controller stirrer and overhead UV irradiation set up was used. The photo catalytic activity of as synthesized nano catalyst was studied by adding 10 mg of the photo catalyst to 100 ml of the 1mM dye solution which was equilibrated in dark for 3hrs before the reaction. The reaction mixture was exposed to UV irradiation using a xenon lamp. The xenon lamp was equipped with a liquid filter to prevent the rise in the temperature due to irradiation. With the beginning of the irradiation the photo degradation of dye solution was initiated and fading of the color of the dye solution indicates the degradation of dye. At regular intervals of time small aliquots of dye solution are siphoned out and visible spectra recorded from the absorbance variation with time data kinetic parameter are derived. The whole procedure was repeated separately each for

the doped ZnO nps- rGO nanocomposites as photo catalyst in each of the photo catalyst experiment.

III. RESULTS AND DISCUSSION

The powder XRD patterns of the undoped and doped ZnO nps in the assynthesised condition measured are presented in **Figure.2**. The XRD patterns tally with the JCPDS file card no 36 – 1451. The diffraction patterns also show that no secondary phases comprising dopant ions are present. The pattern clearly reflects the presence of hexagonal wurtzite phase of ZnO nps for doped ZnO nps also the powder XRD are found in agreement with the mentioned JCPDS file.

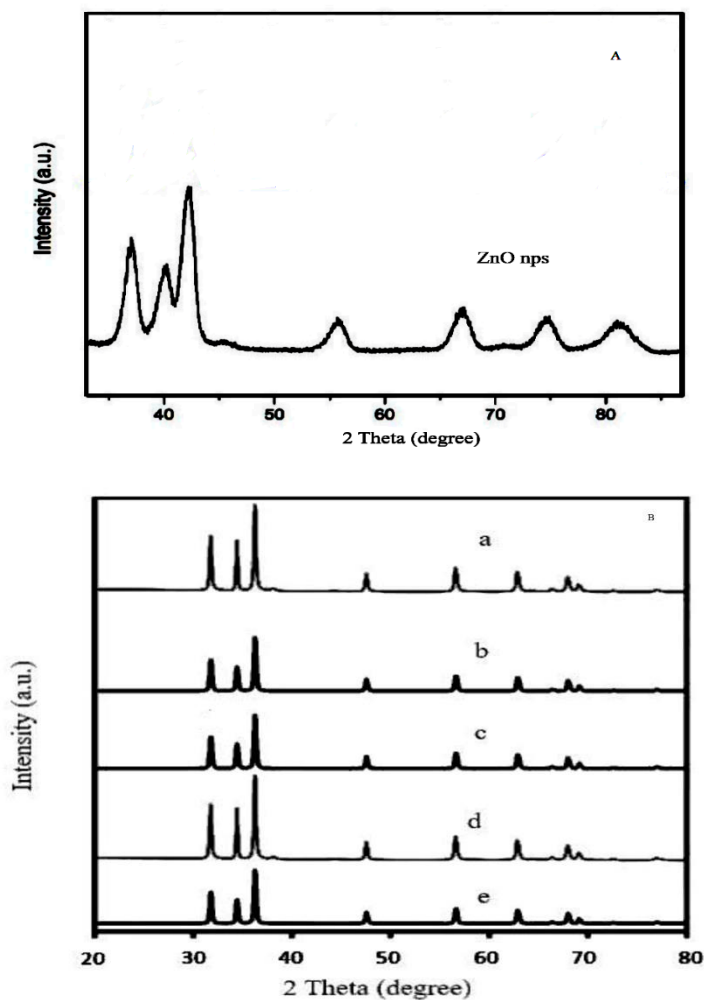


Fig. 2. Powder XRD patterns of (A) ZnO nps and (B) ZnO nps with 5 mol% dopant ions (a) Mg(II); (b) Cu(II); (c) Mn(II); (d) Ni(II); (e) Sb(II) respectively.

The Scherrer formula was used to determine the sizes of nano crystallites of undoped and doped ZnO nps. The HR-TEM photos of undoped and doped ZnO nps and also that of rGO nanocomposites are given in **Figure 3**. The mean particle size values are found out for undoped and doped ZnO nps and are listed in Table.1. These values are in agreement with those calculated from Scherrer equation. Also the TEM photos of the ZnO nps-rGO

nanocomposites indicate the deposition of ZnO nps onto the 2D rGO matrices. The size values in the nanocomposites do not vary much, but well within the % error values of the nano sizes of the pure undoped and doped ZnO nps. **In Table.1**, the mean sizes of the nano crystallites are given. The band gap energy values of both ZnO nps and the metal (II) ion doped ZnO nps are determined from the extrapolation method on the linear relationship between

$(\alpha h\nu)^2$ and $h\nu$, (Tauc plots), where α is the absorption coefficient, k is the proportionality constant and ν is the photon frequency [41]. The band gap values are listed in **Table.1**.

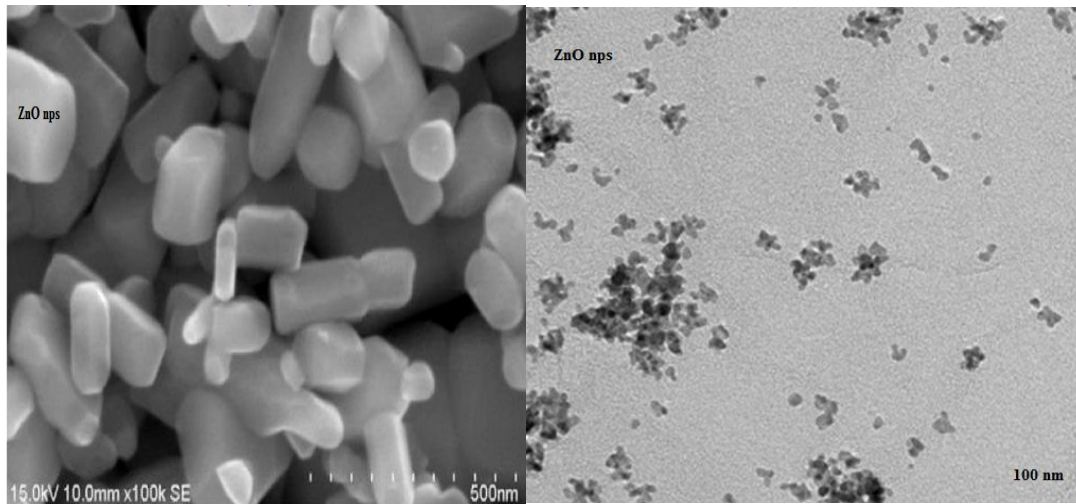


Fig. 3.a. SEM and HR-TEM photos of ZnO nps.

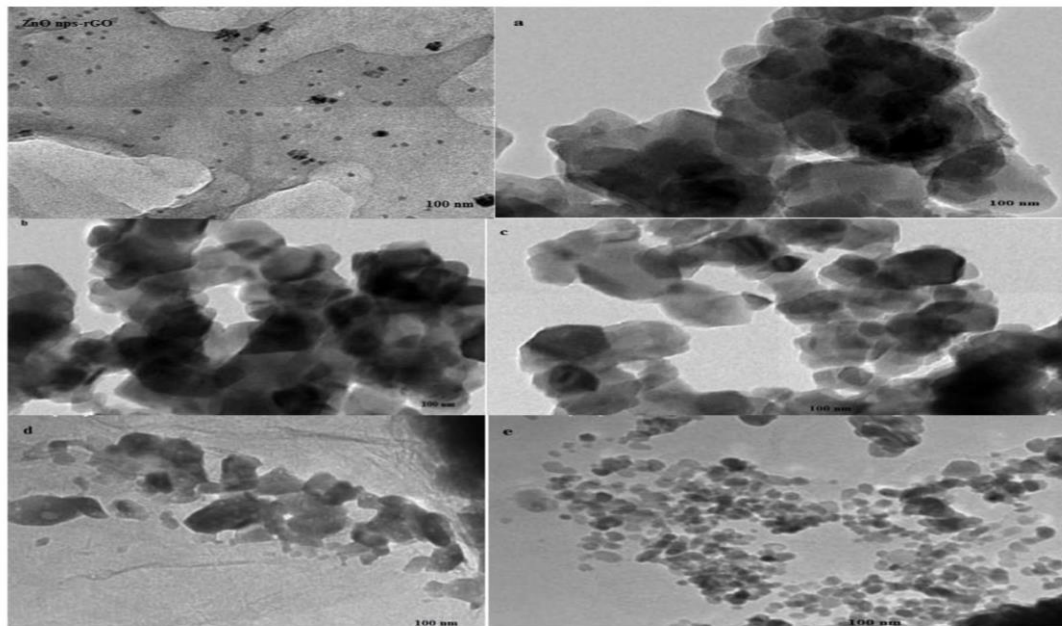


Fig. 3.b. HR TEM photos of ZnO nps-rGO and ZnO nps with 5 mol% dopant ion
 (a) Ni(II); (b) Mn(II); (c) Cu(II); (d) Mg(II); (e) Sb(II)

Table 1. Physical properties [band gap(ev), nano size(nm)] and kinetic parameter-pseudo first rate coefficient ($k \times 10^{-4} s^{-1}$) values of undoped and doped ZnO nps and ZnO nps-rGO nanocomposite

S.No	Nanosystems	Band gap (eV)	Nano size (nm)	Rate constant	% Mineralisation
1.	ZnO nps	3.36	24	6.10	98.0
2.	ZnO nps-rGO	3.27	38	6.26	98.5
3.	Mg(II)-ZnO nps	3.21	42	6.38	98.5
4.	Cu(II)-ZnO nps	3.13	65	6.54	98.8

5.	Mn(II)-ZnO nps	2.95	75	6.95	99.0
6.	Ni(II)-ZnO nps	2.88	78	7.10	99.2
7.	Sb(II)-ZnO nps	3.42	20	5.99	97.5

Undoped ZnO nps exhibit slightly higher value of band gap than that of doped ZnO nps-rGO nanocomposites and as well as that of doped ZnO nps exhibited in **Figure 4**.

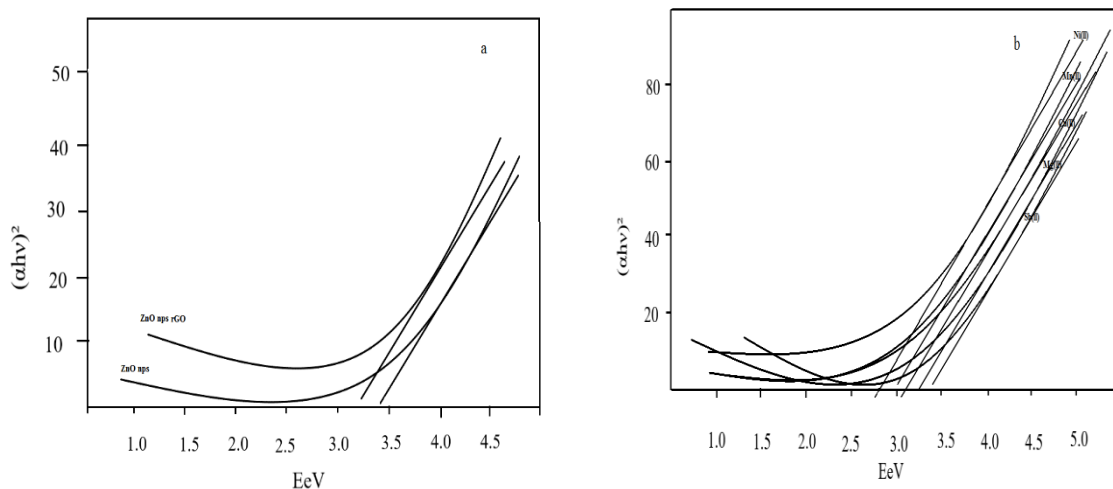


Fig.4. Tauc plots of Aloe vera extract stabilized (a) ZnO nps (b) ZnO nps with 5 mol % dopants Ni(II); Mn(II); Cu(II); Mg(II) and Sb(II) respectively.

In nanocomposites, the reduction in the band gap can be attributed to the presence of Zn-O-C chemical bonds and extended conjugation of unsaturated carbon double bonds and extended conjugation of unsaturated carbon double bonds in the 2 D nanosheets. As the band gap energy is reduced more extents of photons are absorbed by ZnO nps in the nanocomposites, which results in the enhanced photo catalytic activity. Similarly, in the doped ZnO nps, dopants like metal (II) ions are reported to alter the band gap value of undoped ZnO nps [42,43]. By inducing more defects by the presence of minute amounts of dopants which may occupy the Zn(II) vacancy defects, crystallite strain is imparted to a minor extent. Hence due to unit lattice distortions, there may be

a slender loss of crystallinity. This causes the nano size alterations in doped ZnO nps. It was also noted, that when the dopant composition is higher, the photoactivity of ZnO nps decreased. Hence, in this work, 5 mol % composition was maintained for all types of metal (II) dopants, which only exhibited enhancement in the photocatalytic activity. The band gap values are found to be lowered **Table.1.**, except for Sb(II) dopant, where band gap of the doped ZnO nps is marginally higher than the undoped ZnOnps. Also nanocomposite formations with rGO and doped ZnO nps, did not bring down the band gap values deeply, instead only a small extent decrease in the E_g values was noted.

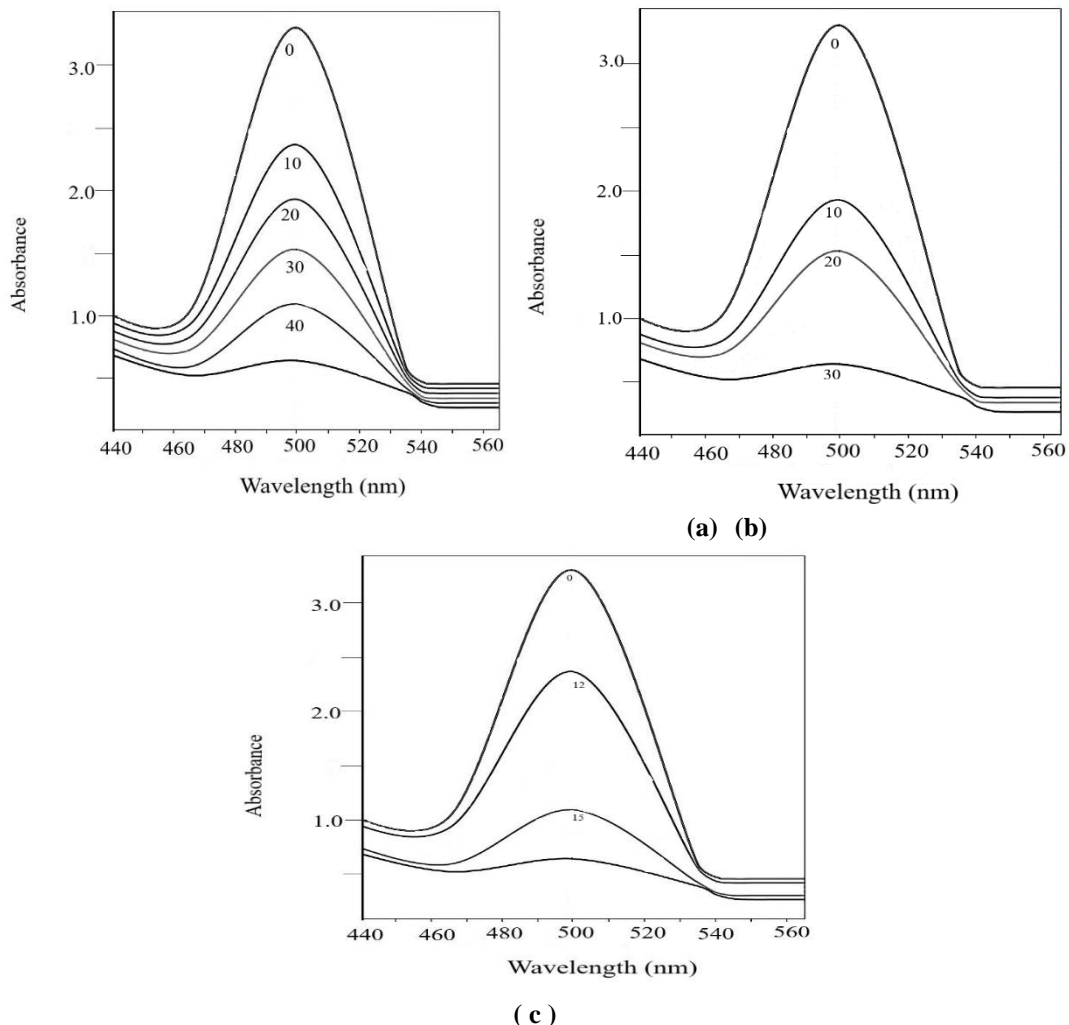


Fig. 5. Visible absorption spectra of 2.0 mM Ponceau 4R dye degradation at intervals of time of photocatalysis with (a) ZnO nps (b) ZnO nps-rGO (c) ZnO nps-rGO with 5 mol % Ni(II) dopant.

Fig.5. presents the time variations in visible spectra of Ponceau 4R dye since the photo catalysis has been initiated in presence of UV light and during the progress of the reaction. As the dye degradation proceeded, fading away of the coloration of dye solution occurred. The extents of the decrease in the absorbances of the characteristic dye absorption peak are higher

with time intervals and as well as in the presence of rGO and doped ZnO nps. From spectral data, absorbance values versus time plots are made for P4R dye degradations in presence of photocatalyst of rGO nanocomposites with pure ZnO nps and doped ZnO nps. Such plots are shown In **Figure.6.**

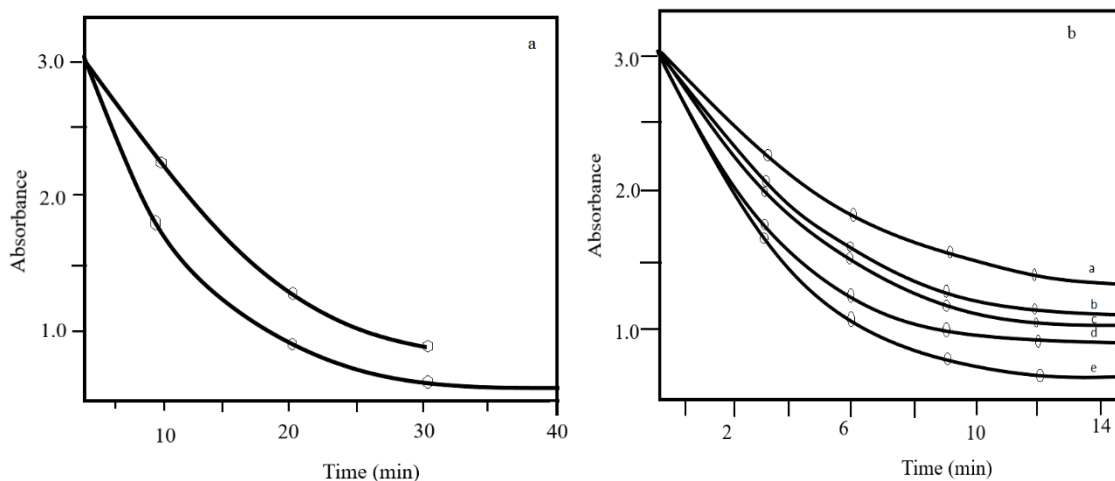


Fig. 6. Absorbance variance with time plots for photocatalytic degradation of Ponceau 4R in presence of (a) Ni(II); (b) Mn(II); (c) Cu(II); (d) Mg(II); (e) Sb(II)

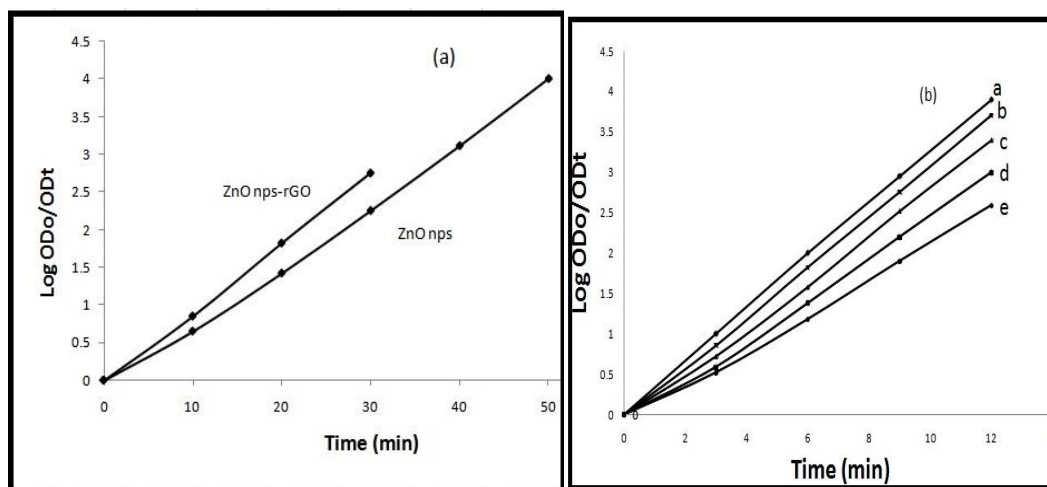
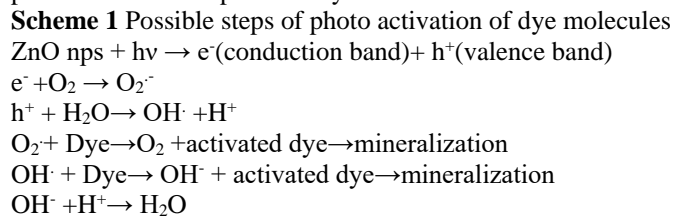


Fig.7. Kinetic plots for pseudo first order rate coefficient determination for photocatalytic degradation of Ponceau 4R in presence of (a) ZnO nps (b) ZnO nps-rGO and ZnO nps-rGO with 5 mol % dopant ions (a) Ni(II); (b) Mn(II); (c) Cu(II); (d) Mg(II); (e) Sb(II)

The overall rate coefficient values of the dye degradation determined in presence of various types of the photocatalysts, have been determined from the linear regressions for zero, first, second and third order kinetic expressions. By doing so, best linear fit was observed for pseudo first order kinetics of the reaction in **Figure.7**. the best fit linear plots of P4R dye degradations in presence of various ZnO nps photocatalysts are given. The rate coefficient values for the pseudo first order rate of the dye degradations in presence of various ZnO nps-rGO photocatalysts are listed in **Table .1**. Kinetic results certainly indicate an enhanced photocatalytic activity in undoped ZnO nps when doped with different metal (II) ions and nanocomposites formations as in ZnO nps-rGO. The enhancement in the photoactivity of ZnO nps-rGO nanocomposites in presence of UV- irradiation may be due to reduction in the recombination process of e^-/h^+ generated. Also quantisations in nanosizes and lowering of band gaps could cause effective transfer of photo electrons on the surface of ZnO nps to

rGO 2D conjugation sheets thereby decreasing the chances of electron-hole recombinations. In the result, compositions of active species like radicals of hydroxyl (OH^\cdot), superoxide ($O_2^{\cdot-}$) are increased and subsequently the dye molecules are activated for rapid degradations. Due to an appreciable increase in the surface area to volume ratio values of ZnO nps during nanocomposite formations with rGO the extents of activation of surface absorbed dye molecules are increased and reflected as rapid decoloration and final mineralization of the dye molecules. In the **scheme 1**, the photo activation steps of the dye molecules are shown.



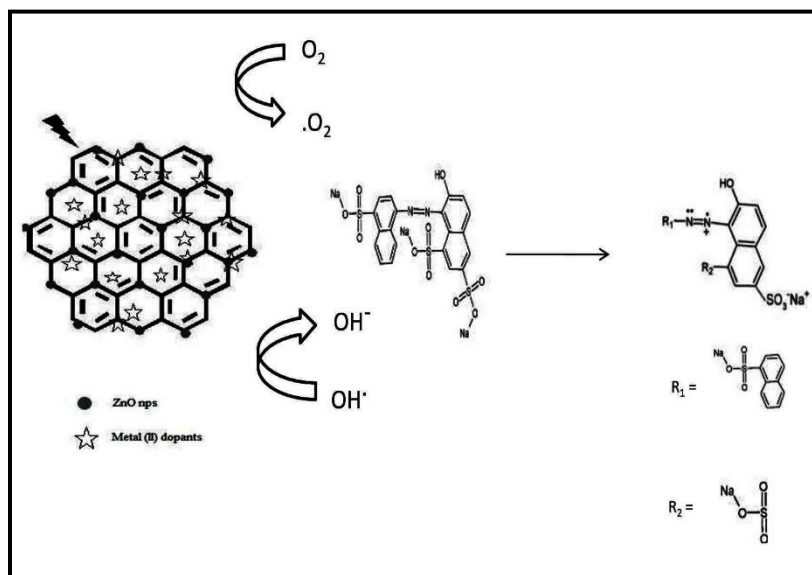


Fig. 8. Mechanism of photodegradation

The dopants such as Mg(II), Cu(II), Mn(II), Ni(II) cause a decrease in the band gap values of ZnO nps, thereby facilitating the photo electrons from valence band to conduction band of ZnO nps and increasing the oxygen vacancies in the nanocrystalline ZnO. Such effects retard the photoelectron and hole recombination resulting in, an enhancement in the photoactivity of ZnO nps. In doped ZnO nps-rGO nanocomposites, photoactivity is increased tremendously. The reasons such as band gap decrease, lattice distortions and increase in defect vacancies can be attributed to the increase in the rate coefficient values of dye degradations in presence of doped ZnO nps-rGO nanocomposites as photocatalysts. However, Sb(II) doped ZnO nps-rGO nanocomposite photocatalyt system did not increase the rate coefficient value is not large compared to other metal(II) dopants. The reduced photocatalytic activity may be due to the slight increase in the band gap value and a small extent in the decrease in the nano size value. These effects increase the photo recombination process rate in the Sb(II) doped ZnO nps-rGO nanosheets, and decreases the availability of photo electron for dye degradations. Hence, photocatalytic efficiency is not enhanced. Among the metal(II) dopants in ZnO nps-rGO composites applied in photocatalysts, Sb(II) dopant did not input enhanced activity in ZnO nps-rGO system.

IV. CONCLUSIONS

Synthesis of undoped and metal(II) doped ZnO nps using, Aloe vera plant extract by green pathway resulted in stable nanosized ZnO nps. Similarly, adopting eco-friendlier hydrothermal conditions and ultrasonication, nanocomposites of undoped and doped ZnO nps-rGO are prepared and characterized. The photo catalytic activities of ZnO nps-rGO nanocomposites are confirmed by studying the photooxidative degradation of dye Ponceau 4R in aqueous medium under UV irradiation. The overall pseudo first order rate coefficient values of the dye degradations in presence of ZnO nps-rGO nanocomposites are determined. In pure ZnO nps, rGO nanocomposites formation decreased the band gap, increased the nano size to a small extent and increased the

rate coefficient value of the dye degradation. Regarding doped ZnO nps with dopants Mg(II), Cu(II), Mn(II), and Ni(II) and the rGO nanocomposites exhibit a decrease in the band gap values, increase in nanosizes and an increase in the rate coefficient values of dye degradation. These effects occur due to a significant suppression in the photo recombination processes in ZnO nps. In case of Sb(II) doped ZnO nps and its rGO nanocomposites, a slight increase in the band gap, a decrease in nano size and a decrease in the rate coefficient of dye degradation are observed. The reason attributed could be due to the extent of suppression in the photo recombination process being not as effective as in the other metal (II) dopants system in ZnO nps. However, all the dopants chosen and rGO nanocomposites of ZnO nps certainly caused an effective photodegradation of water polluting Ponceau 4R dye.

ACKNOWLEDGEMENT

All the authors thank profusely the National Centre for Nanoscience and Nanotechnology, University of Madras, for TEM measurements.

REFERENCES

1. M. Ismail, K. Akhtar, M. I. Khan, T. Kamal, M. A. Khan, A. M. Asiri, J. Seo and S. B. Khan. *Curr Pharm. Des.* 25, 3645-3663, 2019.
2. B. Lellis, C. Z. Fávaro-Polonio, J. A. Pamphile and J. C. Polonio. *Biotechnol Res. Innov.* 3, 275-290, 2019.
3. S. Dong, J. Feng, M. Fan, Y. Pi, L. Hu, X. Han, M. Liu, J. Sun and J. Sun. *RSC Adv.* 5, 14610-14630, 2015.
4. S. Wijetunga, X. F. Li and C. Jian. *J. Hazard. Mater.* 177, 792-798, 2010.
5. M. M. Momeni. *Appl Phys. A: Mater. Sci. Process.* 119, 1413-1422, 2015.
6. M. M. Mahlambi, C. J. Ngila and B. B. Mamba. *J. Nanomater.* 790, 173, 2015.
7. A. Hegazy, E. Prouzet. *Chim.* 16, 651-659, 2013.
8. S. Guo, X. Zhang, Z. Zhau, G. Ga Lu Liu. *Mater. Chem. A* 2, 9236-9243, 2014.
9. Y. Yu. L. Zhang, J. Wang, Z. Yang, M. Long, N. Hu, Y. Zhang. *Nanoscale Res Lett* 7, 347, 1-6, 2012.
10. T. Sreethawong, S. Ngamsinlapasathian, S. Yoshikawa. *Chem. Eng. J.* 228, 256-262, 2013.
11. S. Kant, A. Kumar. *Adv. Mater Lett.* 3, 350-354, 2012.

- [12] 12. Y. Chen, H. Zhao, B. Liu, H. Yang. Appl. Catal. B 163, 189-197, 2015.
- [13] 13. Y. Chen, L. Zhang, L. Ning, C. Zhang, H. Zhao, B. Liu, H. Yang. Chem. Eng. J. 264, 557-564, 2015.
- [14] 14. S. Adhikari, D. Sarkar. G. Madras, RSC Adv. 5, 11895-11904, 2015.
- [15] 15. H. Wang, S. Baek, J. Lee, S. Lim. Chem. Eng 146, 355-361, 2009.
- [16] 16. R. Pawar, D. Choi, J. Lee, C. Lee. Mater. Chem. Phys. 151, 167-180, 2015.
- [17] 17. S. Kuriakose, B. Satpati, S. Mohapatra. Phys. Chem. Chem. Phys. 16, 12741-12749, 2014.
- [18] 18. O. Bechambi, S. Sayadi, W. Najjar. Ind. Eng. Chem. 32, 201-210, 2015.
- [19] 19. Y. Zong, Z. Li, X. Wang, J. Ma, Y. Men. Ceram. Int. 40, 10375-10382, 2014.
- [20] 20. B. Josephine, M. Goodall, D. Illsley, R. Lines, N. Makwana, J. Darr. ACS Comb. Sci. 17, 100-112, 2015.
- [21] 21. J. Tian. et al. Nano Energy 11, 419 -427, 2015.
- [22] 22. A. Molea, V. Popescu, N.A. Rowson, A.M. Dinescu. Powder Technol. 253, 22-28, 2014.
- [23] 23. A. Molea, V. Popescu, N.A. Rowson. Powder Technol. 230, 203-211, 2012.
- [24] 24. Mohd Fadhlan Shah Hermandy, Mohdzakimoha Yuosoff Mohammed Syarifudlu, Mdrabiul Awal. Reviews International Journal of Emerging trends in Engineering Research. 8, 106896-6902, 2020.
- [25] 25. NI Rasli, H Basri and Z Harun, Heliyon 6, 03156, 2020.
- [26] 26. N. Güy, S. Çakar and M. Özacar. J. Colloid Interface Sci. 466, 128-13, 2016.
- [27] 27. J. Rodrigues, T. Hatami, J. M. Rosa, E. B. Tambourgi and L. H. I. Mei. Chem. Eng. Res. Des., 153, 294-305, 2020.
- [28] 28. H. Liu, Y. Hu, Z. Zhang, X. Liu, H. Jia and B. Xu, Appl. Surf. Sci. 355, 644-652, 2015.
- [29] 29. C. Jaramillo-Páez, J. A. Navío and M. C. Hidalgo, J. Photochem. Photobiol. A, 356, 112-122, 2018.
- [30] 30. M. Zayed, A. M. Ahmed and M. Shaban, Int. J. Hydrogen Energy. 44, 17630-17648, 2019.
- [31] 31. S. Kuriakose, K. Sahu, S. A. Khan, A. Tripathi, D. K. Avasthi and S. Mohapatra. Opt. Mater. 64, 47-52, 2017.
- [32] 32. Multi-wall carbon nanotube film-based electrochemical sensor for rapid detection of Ponceau 4R and Allura Red Food Chemistry. 122, 909-913, 2010.
- [33] 33. C. Jaramillo-Páez, J. A. Navío and M. C. Hidalgo, J Sci Food Agric. 91, 2821-2825, 2011.
- [34] 34. E. Forgacs, T. Cserhádi and G. Oros. Environ. Int. Vol. 30, pp. 953-971, 2004.
- [35] 35. H.S. El-Desoky, M.M. Ghoneim and NM Zidan., Desalination Vol. 264, pp. 143-150, 2010.
- [36] 36. S. Kuriakose, K. Sahu, S. A. Khan, A. Tripathi, D. K. Avasthi and S. Mohapatra. International Journal of Innovative Research in Science, Engineering and Technology , Vol. 3, Issue 2, February 2014.
- [37] 37. A. Ojha, P. Thareja. Appl. Surf. Sci. 435, 786-798, 2018.
- [38] 38. H. Kim, G. Moon, D. Monllor-Satoca, Y. Park, W. Choi. J. Phys. Chem. C 116, 1535-1543, 2012.
- [39] 39. I. Poullos, E. Micropoulou, R. Panou, E. Kostopoulou. Appl. Catal. B Environ. 41, 345-355, 2003.
- [40] 40. W.S. Hummers, R.E. Offeman. J. Am. Chem. Soc. 208, 1937, 1957.
- [41] 41. Marilyn Yuen Sok Wen, Abdul Halim Abdullah, Lim Hong Ngee. Malaysian Journal of Analytical Sciences., 21 No 4, 889 – 900, 2017.
- [42] 42. Lv, T., Pan, L., Liu, X., Lu, T., Zhu, G and Sun, Z. Journal of Alloys and Compounds, 509(41), 10086 – 10091, 2011.
- [43] 43. Nipane, S., Korake, P. and Gokavi, G. Ceramics International, 41 (3), 4549 – 4557, 2015.

AUTHORS

First Author – R. Vijayalakshmi, Department of Chemistry, Quaid E Millath Government College for Women, Annasalai, Chennai 600 002, TamilNadu, India

Second Author – L. Ramapriya, Department of Chemistry, Dr.M.G.R Educational and Research Institute, Chennai 600 095, TamilNadu, India

Third Author – J. Santhanalakshmi, Department of Physical Chemistry, University of Madras, Maraimalai Campus, Chennai – 600 025 (Retd.)

Correspondence Author – Tel : 9282145310; E-mail : vijiradha68@gmail.com